A DIGITAL MODEL OF PART OF THE RIO TEMPISQUE ALLUVIAL AQUIFER, COSTA RICA

D. Mora-Castro* and J. W. Lloyd†

ABSTRACT

The hydrogeology of the area is discussed and the method used in producing a digital model simulation of the alluvial aquifer is described. The availability of groundwater resources in the area is indicated by modelled areal abstractions and drawdown modified by a simple 'worst well' concept of well interference and well loss. Introducing this concept reduces the postulated allowable areal abstraction in the study area by 50 percent.

INTRODUCTION

The Rio Tempisque is situated in western Costa Rica, along the north-eastern border of the Nicoya Peninsula. It flows southwards to the Gulf of Nicoya on the Pacific Ocean and drains the northern part of the peninsula and a major part of the Cordillera del Guanacaste. Volcanic mountains in the Cordillera rise 3500 m above sea level, while in the west the catchment is separated from the Pacific by a chain of low hills of up to 300 m elevation. The central part of the catchment is a broad, mature undulating valley generally about 50–100 m in elevation and is of considerable agricultural importance. A regional location map of the area is shown in Fig. 1.

The climate of the area is tropical, with the main rainfall season occurring from May to November. The highest precipitation falls in the Cordillera del Guanacaste, where at Quebrada Grande in the upper Rio Tempisque annual rainfall totals are recorded ranging between 1966 and 2372 mm (1968–1973). At Filadelfia, the chief agricultural town in the central part of the valley, annual totals range between 1370 and 2420 mm (1950–1973). The precipitation sustains perennial flows in the Rio Tempisque.

REGIONAL GEOLOGY

The geology of the area is shown on Fig. 2. The valley of the Rio Tempisque forms part of a down-thrown fault block related to Plio-Pleistocene movements (Mora-Castro, 1974). Within the valley extensive alluvial sediments have been deposited on a complex of Quaternary, Tertiary and Mesozoic rocks. From a water-supply and hydrogeological point of view the alluvium is of major

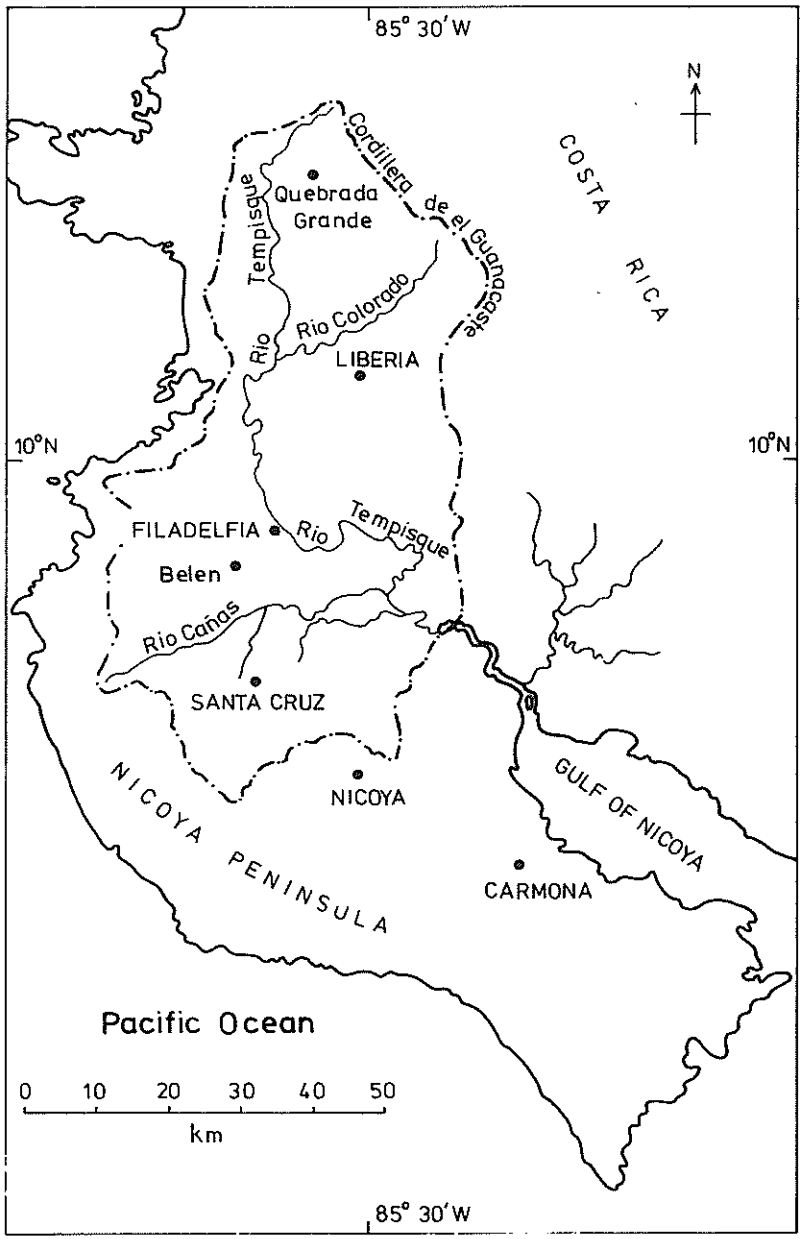

FIG.1 — Location map of the Rio Tempisque catchment.

water-bearing importance, although the older rocks are significant with respect to boundary conditions.

Of the geological units shown on Fig. 2, the Mesozoic rocks occur chiefly in the west and north of the area and are composed mainly of lavas and greywackes with basic intrusions. In the southeast a sequence of Upper Cretaceous to late

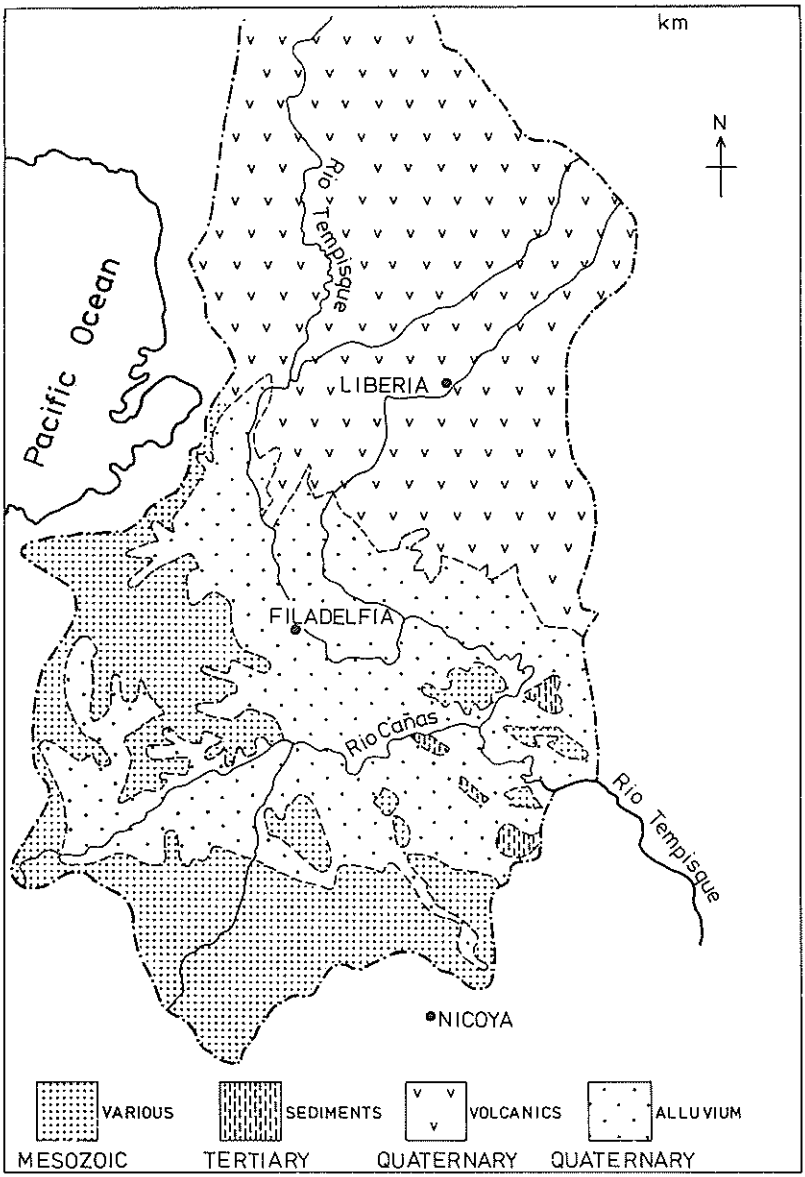

FIG.2 – Geological map of the Rio Tempisque catchment.

Tertiary limestones, tuffaceous sandstones, and conglomerates are present. The rest of the area is underlain by Quaternary lavas and pyroclastic rocks.

The central valley area of the Rio Tempisque is covered by poorly sorted alluvium derived from the older rocks. Grain sizes decrease generally from the alluvial margins to the centre of the valley, although gravels, sands, silts and clays may be interbedded throughout. In the vicinity of Filadelfia along the eastern side of the Rio Tempisque fine-grained sediments predominate with important implications on groundwater movement. The thickness of the sediments is variable ranging from a feather edge at the margins up to 600–100 m in the centre of the valley.

The Mesozoic rocks yield minor groundwater supplies but are generally unproductive, while the Quaternary volcanics which are present in the high rainfall areas provide a major surface-water contribution to the Rio Tempisque.

WATER SUPPLY PROBLEMS

The main population and agricultural interests in the region are concentrated in the central part of the Rio Tempisque valley in the area to the west of the river between Sardinal, Filadelfia and Belen. Water supply is important with respect to population requirements, irrigation and stock watering. Perennial surface water is used but is variable in volume and has been completely allocated through the existing water rights and licensing procedures. To alleviate water in areas away from the river and to allow further agricultural development in the savannahs to the west of Filadelfia, studies have been implemented to assess the availability of groundwater in the alluvium. Standard groundwater investigations have been carried out, and the initial possible development of the resources has been examined using a digital groundwater model of an area of approximately 350 km^2.

HYDROGEOLOGY OF THE ALLUVIUM

For the purposes of the resources investigation, the alluvium in the area shown on Fig. 3 has been studied with respect to water levels, boundary conditions, aquifer characteristics and recharge.

In the area depicted, the alluvium overlies Mesozoic rocks which are essentially impermeable so that a lower impermeable boundary is defined at the base of the alluvium. The aquifer is unconfined, with a westerly flow to the Rio Tempisque as illustrated by the water-table map shown on Fig. 3. The presence of fine-grained alluvium to the east of the Rio Tempisque provides a lateral, essentially impermeable limit to the aquifer which for practical purposes has been taken to coincide with the river (see schematic geological section on Fig. 3). Along this boundary the groundwater is effluent to the river which reflects the head in the aquifer. The western boundary of the aquifer is the feather edge of

* Servicio Nacional de Aguas Subterraneous, Apartado 5262, San Jose, Costa Rica.
† Department of Geological Sciences, University of Birmingham, P.O. Box 363, Birmingham B15 2TT, England.

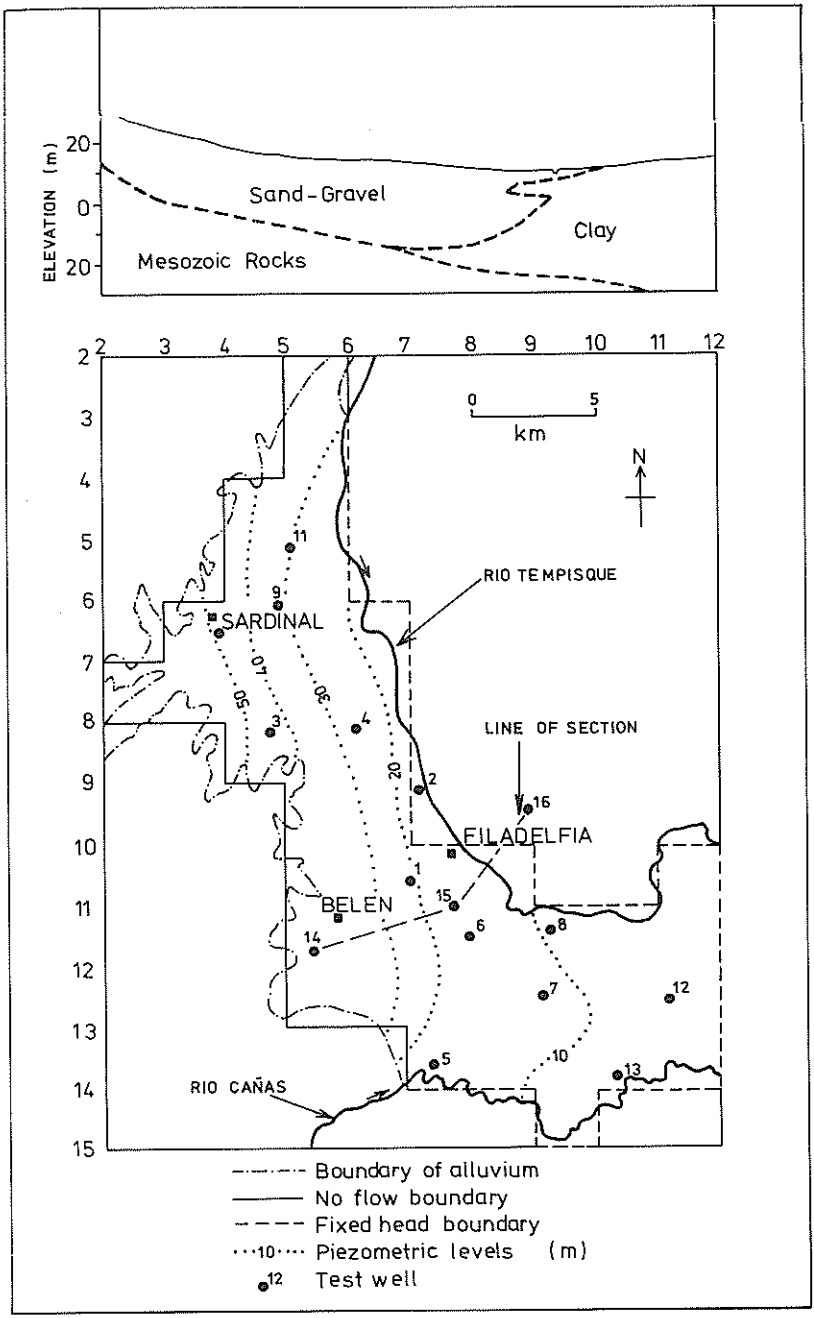

FIG.3 – Geometry of area selected for model.

the alluvium where it overlies the Mesozoic impermeable rocks. Flow into the alluvium is via surface runoff in streams draining Mesozoic outcrops and direct recharge from rainfall.

To determine the hydraulic characteristics of the aquifer, pumping tests were carried out on existing wells in the area and at 13 especially constructed test sites. Data analysis was carried out using Boulton (1963) unconfined-type curves. The transmissivities and specific yields obtained are listed in Table 1, and the bore hole distribution is shown on Fig. 3.

In order to determine recharge, well hydrographs were analysed as depicted on Fig. 4. Composite regression curves were established for each monitored well by integrating a range of hydrograph recessions. At a particular time interval the

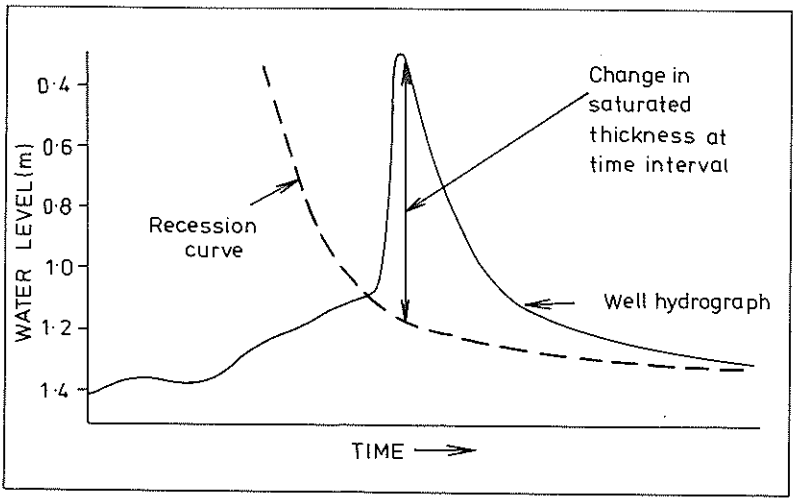

FIG.4 – Hydrograph analysis related to recharge estimates.

TABLE 1 – Aquifer parameters from pumping-test data.

Well No.	*Well depth (m)*	*Transmissivity (m^2/day)*	*Special Yield (%)*
1	61.0	1700	0.15
2	30.7	1500	0.10
3	18.25	590	0.14
4	70.10	685	0.10
5	3.05	10	0.03
6	42.36	325	0.08
7	43.89	–	0.06
8	50.30	2920	0.20
9	50.90	1950	0.08
10	61.0	1639	0.08
11	58.82	–	0.05
12	34.13	102	0.06
13	29.87	330	0.06

saturated thickness was determined by subtracting the water level established by the composite curve from the actual water level shown on the hydrograph. The saturated thickness was then multiplied by the specific yield and the area of influence of the well as determined by a Thiessen polygon distribution, to estimate the volume of recharge to the aquifer.

DIGITAL MODEL THEORY

Having established acceptable basic parameters for the aquifer, a simulation of the aquifer was obtained based on the equation adopted by Walton (1970) which describes the time-variant drawdown throughout an aquifer when the vertical components of flow are considered sufficiently small to be neglected.

$$\partial/\partial x\,(T_x \partial s/\partial x) + \partial/\partial y\,(T_y \partial s/\partial y) = S\partial s/\partial t + Q \qquad (1)$$

where T_x and T_y are the transmissivities in the x and y direction, s is the drawdown, S is the specific yield of the aquifer in this case, and Q is the quantity of water entering the aquifer per unit area per unit time. Since the aquifer is assumed to be isotropic but non-homogeneous, values of T_x at T_y at a point will be equal. The subscripts x and y are introduced here to facilitate the development of a finite-difference approximation to the non-homogeneous case. It is assumed that the non-homogeneity is small and that equation (2) adopted below can be written with no loss of accuracy. In this respect for a practical solution of equation (1), time and space dimensions were divided into discrete intervals after Pinder and Bredehoeft (1968) throughout the aquifer system, and for the finite difference approximation a backward difference approach was adopted (Rushton, 1973) in which

$$T_x \partial^2 s_{n+1}/\partial x^2 + T_y \partial^2 s_{n+1}/\partial y^2 = S\,(s_{n+1} - s_n)/\Delta t + Q_{n+1/2} \qquad (2)$$

With this approximation the space derivative is centred at a time $(n+1)\,\Delta t$ and the time derivatives at time $(n+\tfrac{1}{2})\,\Delta t$. For computational purposes the aquifer is divided into a grid with a nodal distribution $(s_{i,j})$ as shown on Fig. 5 and equation (2) is given as

$$T_{x,i,j}\,[(s_{i+1,j} - 2s_{i,j} + s_{i-1,j})/\Delta x^2]_{n+1} + T_{y,i,j}\,[(s_{i,j+1} - 2s_{i,j} + s_{i,j-1})/\Delta x^2]_{n+1}$$

$$= S\,(s_{i,j,n+1} - s_{i,j,n})/\Delta t + Q_{i,j,n+1/2} \qquad (3)$$

The boundary condition of a 'fixed head' is applied directly by retaining the appropriate head at the specified value. For an impermeable boundary, the condition of 'no flow' crossing the boundary $s/y = 0$ is applied through a fictitious node $i,j+1$ by setting $s_{i,j+1} = s_{i,j-1}$; further details of the configurations are discussed below. The finite-difference approximations lead to a large number of simultaneous equations which were solved using iterative over-relaxation techniques (Rushton, 1974).

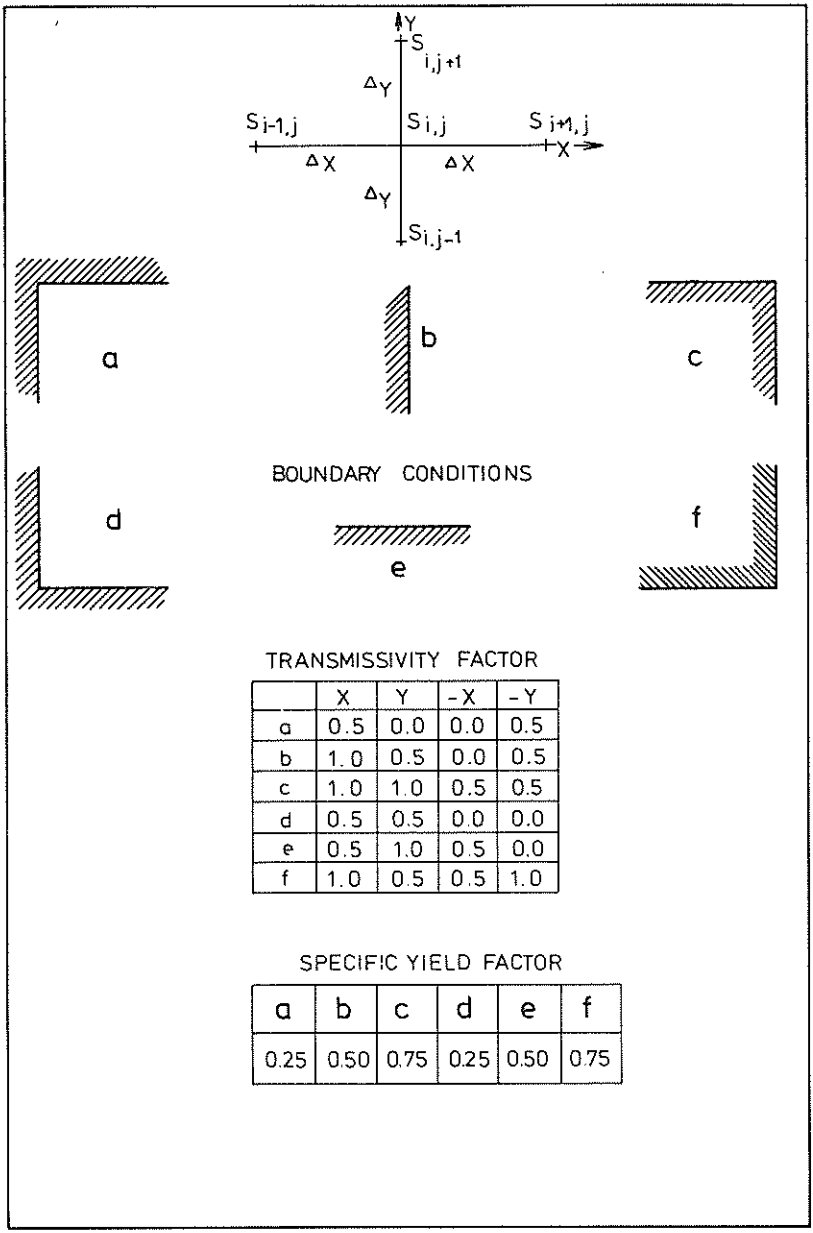

TRANSMISSIVITY FACTOR

	X	Y	-X	-Y
a	0.5	0.0	0.0	0.5
b	1.0	0.5	0.0	0.5
c	1.0	1.0	0.5	0.5
d	0.5	0.5	0.0	0.0
e	0.5	1.0	0.5	0.0
f	1.0	0.5	0.5	1.0

SPECIFIC YIELD FACTOR

a	b	c	d	e	f
0.25	0.50	0.75	0.25	0.50	0.75

FIG.5 – Boundary modification factors.

PRACTICAL MODEL CONSTRUCTION AND AQUIFER SIMULATION

To construct the model the area was subdivided on a grid as shown in Fig. 3, with grid intersections representing data-input nodes equally spaced at 2.5-km intervals. The area of influence for each node is a square 2.5 × 2.5 km based on the node as a centre point. Using the basic data obtained from field studies, namely transmissivity, specific yield, recharge and groundwater level, values were selected for each adjacent nodal pair. In the non-boundary affected nodal areas these values were balanced with surrounding nodal areas using the groundwater flow equations discussed above. Where boundaries were present, two different approaches were used. The western boundary of aquifer was determined as a boundary of 'no flow', and the eastern boundary as a 'fixed head' boundary along the river in view of the hydraulic continuity between the river and the aquifer.

For those nodal pairs affected by 'no flow' boundaries, transmissivities were multiplied by a factor as shown on Fig. 5. These factors allow for groundwater flow to be modified in a particular direction in proportion to the amount of 'no flow' boundary influencing a nodal area. A similar technique was applied to specific yield values using the factors also shown on Fig. 5. Recharge data in the boundary affected areas were determined in proportion to the actual aquifer area present.

To obtain an aquifer simulation, the model was programmed to accept four years of recharge data on a monthly basis for the period 1969–1973. The simulation was attained both in time, and spacially as shown on Fig. 6. Initial conditions for the simulation were obtained by running the model for four years of five cycles with identical four-year recharge and boundary head data for each cycle. The results at the end of the fourth and fifth cycles were identical and considered suitable for simulation.

MODELLED ABSTRACTION

In order to estimate the magnitude of allowable abstraction from the aquifer within the area, operation was undertaken using the four-year recharge-cycle data as no other data were available. The relationship of this recharge cycle to long-term data has been assessed on the basis of precipitation statistics. Data for the central part of the valley of the Rio Tempisque show that the 1953–73 mean is 93.4 percent of the four-year average. The percentage difference indicates that the four-year period is reasonably representative of past rainfall conditions, so that abstraction based on such a steady state cycle should produce initial acceptable estimates of long-term aquifer response and water level change, providing adequate safety limits are applied.

To simulate abstraction, negative values of Q were applied to nine nodes indicated on Fig. 6. In accordance with the water supply needs of the area, abstraction was simulated separately for four different rates 0.6, 1.2, 2.4, and 6 $10^6 m^3$ per annum per node. In proportioning seasonal abstraction from individual nodes, account was taken of the nodal transmissivity and the period of the year, the latter being graded between maximum and minimum values as shown in the example in Table 2. Abstraction was simulated only after steady state conditions were established on the cyclic pattern.

As an example, the groundwater level drawdown obtained at node 5–5 for the various overall abstraction rates is given in Fig. 7. This node represents the maximum drawdown conditions encountered in the study.

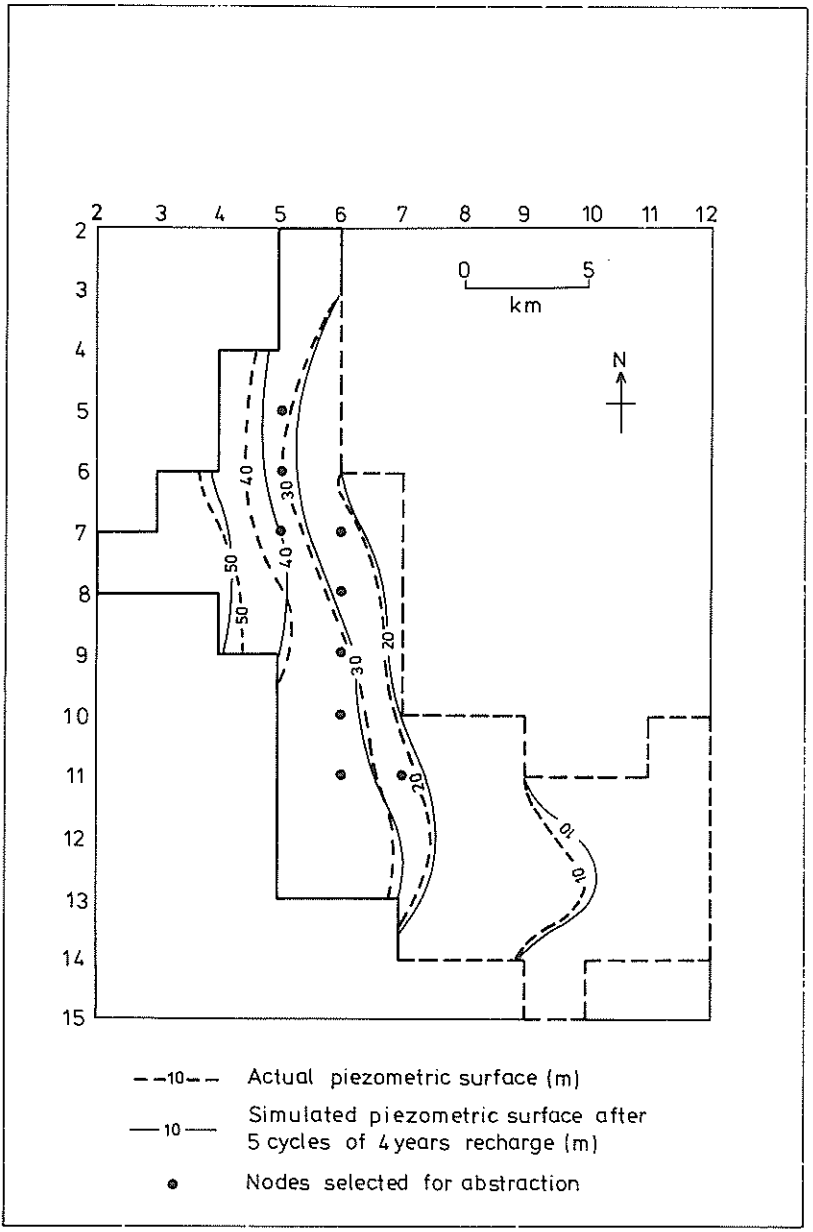

FIG.6 – Simulated piezometric surface.

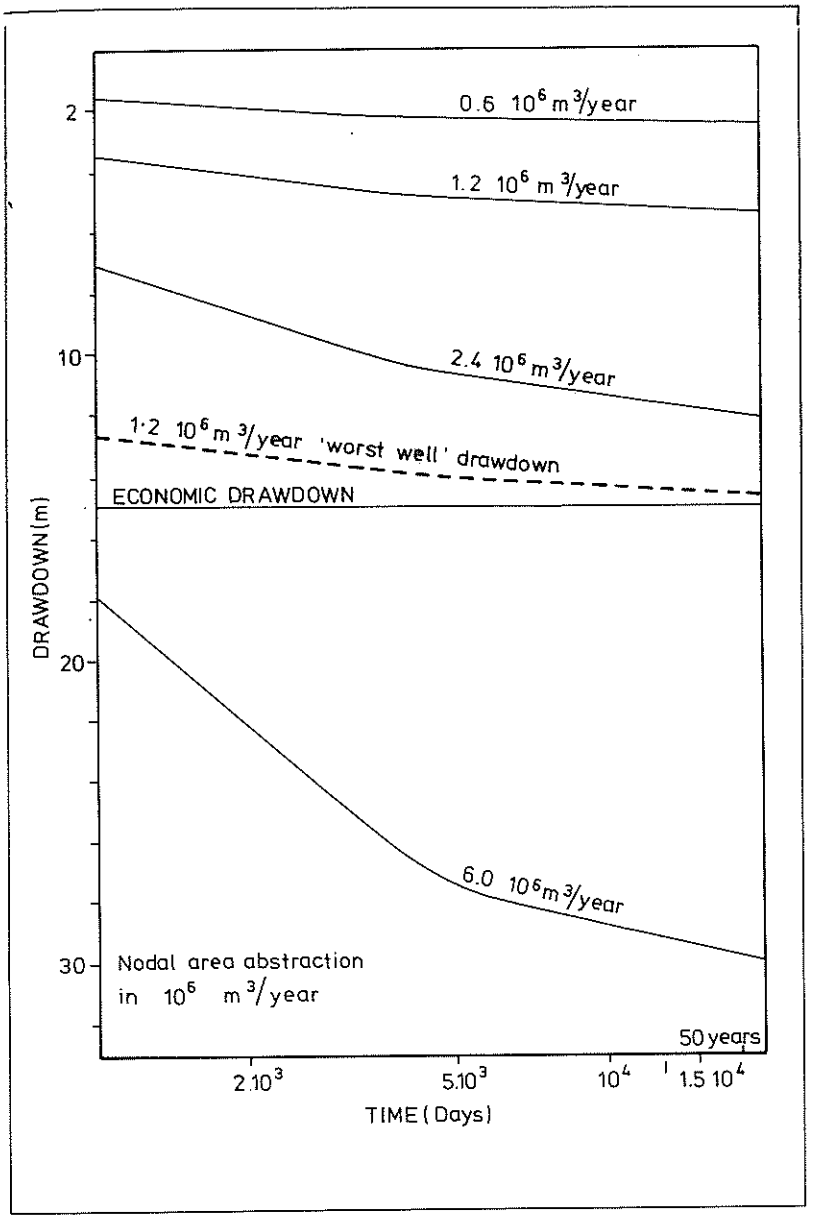

FIG.7 – Time-drawdown relationships for various abstractions at mode 5–5 with 'worst well' drawdown at 1.2 $10^6 m^3$/year in well field.

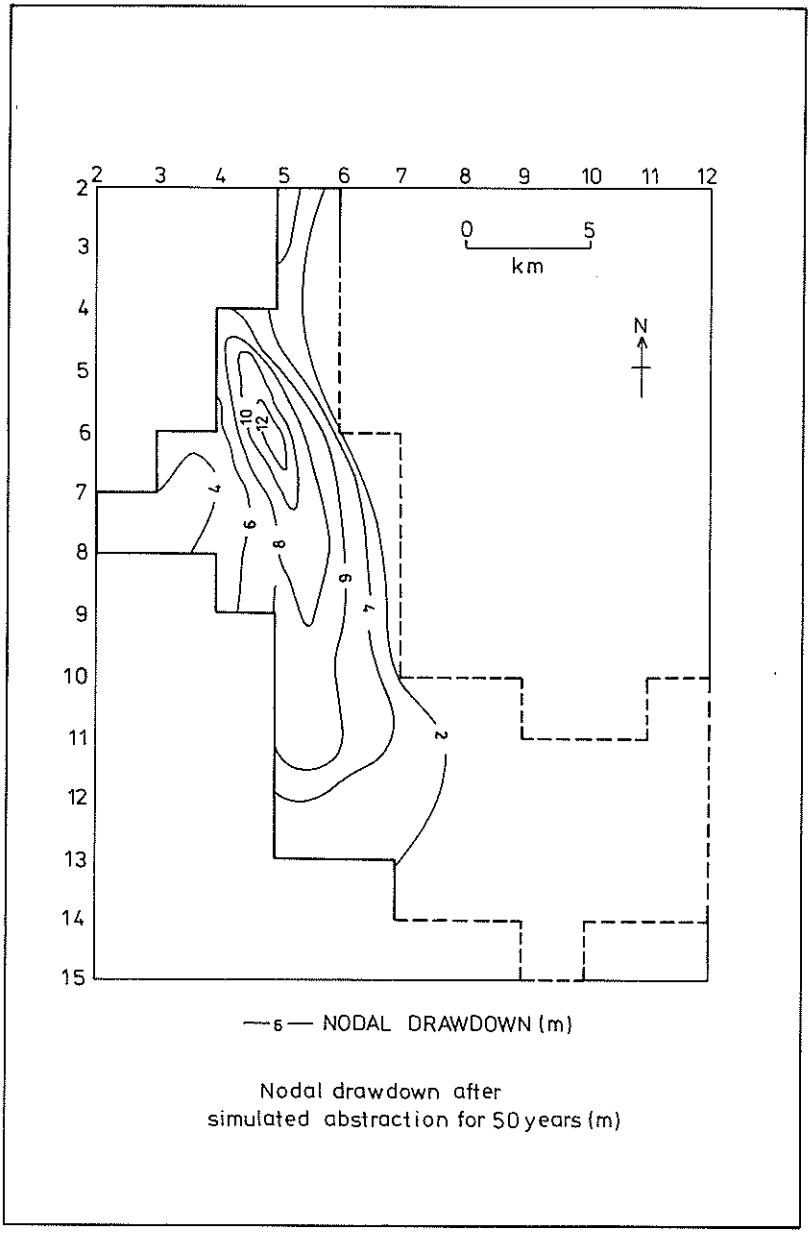

FIG.8 – Simulated regional drawdown of 1.2 $10^6 m^3$/year.

TABLE 2 – Example of individual nodal astraction rates.

Node co-ordinates	*Transmissivity (m^2/day)*	*Max. pumping rate (m^3/day)*	*Min. pumping (m^3/day)*
5– 5	695	1.3210^3	0.0
6–10	3035	2.6410^3	0.0

The regional nodal area drawdown response is shown on Fig. 8. From Fig. 7 as a preliminary approximation it would appear that the aquifer could support an abstraction rate of 2.4 $10^6 m^3$ per annum per node if the agricultural economic drawdown criterion of about 15 m below water table for the area is applied. The value of 15 m of drawdown is based on an estimate of the average drawdown operated by farmers in the region at present. This value is somewhat subjective, but can be modified as new data become available. It provides, however, a workable starting point.

The nodal area drawdown trends shown on Fig. 7 do not allow for well interference effects and well loss. In order to assess these factors, a well field was constructed for the area and interference between wells assessed using traditional non-steady time-yield-drawdown techniques (Wenzel, 1942). All wells were assumed to be fully penetrating. The optimal well distribution within the well field was determined on a square grid pattern with the distances between wells determined on a trial-and-error basis. Well yields comparable to those already existing in the area were used, and various field constructions were made to obtain the four bulk abstractions simulated on a nodal area basis. Well loss values for the area were obtained (Jacob, 1947) and the concept of a 'worst well' condition was applied. In the well field the well with the maximum drawdown attributed to interference and point drawdown at the well itself was determined. A well loss value was added, and this well defined as the 'worst well'. The total drawdown thus obtained was used to correct the position of the nodal drawdown trend as a function of the time-drawdown performance of the 'worst well' within the nodal area. In establishing the interference and point drawdown effects, values after 24 hours were totalled. This period is about twice that required to attain virtual steady-state conditions in wells in the area. Thus, using the non-steady-state drawdown, an adequate drawdown safety factor is introduced. In adopting the simplified 'worst well' concept the extremely difficult finite-difference modelling techniques of rapid large drawdown changes typified by a pumping well (Rushton, 1973) are obviated and a practical maximum point drawdown within an area can be estimated for the purposes of initial aquifer response assessment. Further, the sophistication of a modelled well-field abstraction programme is not warranted on the basis solely of an initial regional aquifer model.

In the study area the introduction of 'worst well' drawdown data indicates that rather than an abstraction of 2.4 $10^6 m^3$ per annum per node being allowable under the criteria stated, a more realistic abstraction of the order of 1.2 $10^6 m^3$ per annum per node should be considered initially, as depicted by Fig. 7.

CONCLUSIONS

The authors consider that the approach discussed provides a reliable initial assessment of the groundwater resource availability of the area studied. The data processed and the method used produce an adequate simulation of the aquifer conditions.

Drawdown based on nodal area abstraction requires modification to take into account well-field interference and well loss. Without, however, a comprehensive knowledge of water use requirements and an agro-economic study backed by further hydrogeological work, only a simple approximation is required or indeed justified. The simple 'worst well' concept is considered sufficient for this level of study and emphasises the importance of the various drawdown elements within a nodal area by reducing the postulated allowable nodal area abstraction by 50 percent. Obviously, well fields and abstraction can be modified for optimal drawdown conditions but the technique establishes the order of abstraction.

For further study a trial development project is recommended so that the aquifer can be tested and the model up-graded against significant bulk abstraction of the order of 1 $10^6 m^3$/year for three years from one nodal area. Decisions on major development can follow this later phase.

ACKNOWLEDGMENT

The authors would like to thank the Servicio National de Aguas Subterranean of Costa Rica for supplying the basic data for the study and for kindly giving permission to publish this paper.

REFERENCES

Boulton, N.S. 1963: Analysis of data from non-equilibrium pumping tests allowing for delayed yield from storage. *Proceeding of the Institution of Civil Engineers 29:* 469-482.

Jacob, C. E. 1947: Drawdown test to determine effective radius of artesian well. *Transactions of the American Society of Civil Engineers 112:* 1047-1070.

Mora-Castro, D. 1974: Digital computer model of the Rio Tempisque alluvial aquifer, Costa Rica. M.Sc. Thesis. Department of Geological Science, University of Birmingham, England. 40 p.

Pinder, G. F.; Bredehoeft, J. D. 1968: Applications of the digital computer for aquifer evaluation. *Water Resources Research 4:* 2069-1093.

Rushton, K. R. 1973: Discrete time steps in digital computer analysis of aquifers containing pumped wells. *Journal of Hydrology (Netherlands) 18:* 1-19.

Rushton, K.R. 1974: Critical analysis of the alternating direction implicit method of aquifer analysis. *Journal of Hydrology (Netherlands) 21:* 153-172.

Walton, W. C. 1970: *Groundwater Resource Evaluation.* McGraw-Hill, New York. 664 p.

Wenzel, L. K. 1942: Methods for determining permeability of water bearing materials with special reference to discharging well methods. *U.S. Geological Survey Water Supply Paper 887.* 192 p.